Biophysical Journal, Volume *114*

Supplemental Information

HullRad: Fast Calculations of Folded and Disordered Protein and Nucleic Acid Hydrodynamic Properties

Patrick J. Fleming and Karen G. Fleming

Supporting Information

HullRad: Fast Calculations of Folded and Disordered Protein and Nucleic Acid Hydrodynamic Properties

Patrick J. Fleming and Karen G. Fleming

(2018) *Biophysical Journal*
https://doi.org/10.1016/j.bpj.2018.01.002

T. C. Jenkins Department of Biophysics, John Hopkins University, Baltimore, MD 21218, USA

1 Theory 2
1.1 Stokes-Einstein equations 2
1.2 Hydration water considerations 2
1.3 Effective hydration layers are different for translational and rotational diffusion 3
1.4 The effects of shape are different for translational and rotational diffusion 4
2 Supplemental Figures 5
2.1 Supplemental Figure 1 5
2.2 Supplemental Figure 2 6
2.3 Supplemental Figure 3 7
2.4 Supplemental Figure 4 8
2.5 Supplemental Figure 5 9
3 Supplemental Tables 10
3.1 Supplemental Table 1 10
4 References 11

1 Theory

1.1 Stokes-Einstein equations

The anhydrous diffusion coefficients of a molecule in solution are related to the equivalent size, anhydrous sphere by the Stokes-Einstein equations,

$$D_T = \frac{k_B T}{6\pi\eta_0 R_0} \tag{S1a}$$

$$D_R = \frac{k_B T}{8\pi\eta_0 R_0^3} \tag{S1b}$$

where D_T is the translational diffusion coefficient, D_R is the rotational diffusion coefficient, k_B is the Boltzmann constant, T is temperature, η_0 is the solvent viscosity, and R_0 is the radius of the equivalent size, anhydrous sphere.

For a protein or nucleic acid in solution the operative radius is not the radius, R_0, of a sphere equivalent to the anhydrous volume of the molecule, but rather the equivalent radius, R_H, of the hydrated molecule that includes any waters of hydration that transiently interact with the molecule and affect its diffusion, times a shape factor, F_S, to account for non-sphericity. As discussed below, both the hydrated radii and the shape factors are different for translational and rotational diffusion.

1.2 Hydration water considerations

The amount of hydration water, and therefore the expansion of R_H over R_0, has been a controversial topic. Kuntz and Kauzmann originally reviewed this topic and concluded that proteins may have between 0.3 and 0.6 grams of hydration water per gram of protein (1). Importantly, different proteins appear to have different apparent fractions of hydration water. This fact means that assumption of a uniform hydration fraction in the calculation of hydrodynamic properties would lead to variable errors depending on the specific protein. To account for hydration when calculating hydrodynamic coefficients from structure, various approaches have been employed, and most use an empirically derived best-fit uniform value for the hydration. In the boundary element method, the triangulated protein surface is expanded by some thickness optimized for all proteins in a data set (2). In the bead-modeling method the size of the beads is expanded to some radius also optimized for all proteins in the data set (3, 4) or molecular dynamics simulations may be used to identify specific hydration waters that are then used in the calculation (5). In an ellipsoid model a hydration layer equal to the diameter of a water molecule (2.8 Å) is added to the surface of the ellipsoid (6). And for the numerical path integration method individual residues are modeled as expanded spheres to account for hydration (7).

Such adjustments for hydration water imply that this water is rigidly bound to the surface of the protein and increases its apparent size. However, the diffusion rate of surface water has been shown by both computational (8) and experimental methods (9) to be orders of magnitude greater than the protein. Therefore, significant hydration water is

not rigidly bound to the surface of the protein. This apparent paradox may be reconciled by assuming that the hydration waters transiently interacting with the protein surface experience a modest viscosity enhancement (10).

In addition to the *hydration* waters described above, which may be considered an inherent part of the macromolecule, some water is also likely to be *hydrodynamically* part of the diffusing particle due to the shape irregularities of the macromolecule. There is evidence that water flow in surface crevices of irregularly shaped particle aggregates (analogous to the surface crevices on proteins or the major groove around DNA duplexes) is retarded (11). This latter situation would make the fraction of apparent hydration partially dependent on the shape and size of surface crevices. As stated by Tanford, "…sharp indentations on the surface, will naturally contain solvent, and…this "trapped" solvent will travel with the same velocity as the adjoining macromolecular substance…" (12) (cf. Figures 2, 8 and 9 in the main text).

1.3 Effective hydration layers are different for translational and rotational diffusion

A frequently unappreciated aspect of hydration water is that the hydration layer has different effects on translational and rotational diffusion (1). In order to correctly model the hydration layer in calculations of diffusion coefficients this difference must be taken into account. Consideration of the varied solvent velocities around a translating and rotating sphere explains the origin of this difference (13). The velocity components of a solvent molecule for the case of translational diffusion may be visualized as in Supplemental Figure 1 (adapted from (13)).

The apparent velocity of solvent at any point r around a sphere of radius R during translational diffusion at low Reynolds number conditions can be described by two vectors, v_r and v_θ,

$$v_r = v_\infty \left[1 - \frac{3}{2}\left(\frac{R}{r}\right) + \frac{1}{2}\left(\frac{R}{r}\right)^3\right] cos\theta \tag{S2a}$$

$$v_\theta = v_\infty \left[-1 + \frac{3}{4}\left(\frac{R}{r}\right) + \frac{1}{4}\left(\frac{R}{r}\right)^3\right] sin\theta \tag{S2b}$$

where v_∞ is either the velocity of the sphere in stationary bulk solvent or the velocity of the bulk fluid around a stationary sphere. The relative velocity of fluid at $r = R$ is zero (stick boundary conditions), and approaches v_∞ as $1/r$ moving away from the surface.

For rotational diffusion only, the solvent angular velocity at point r, relative to the sphere surface, is equal to,

$$v_\emptyset = v_\Omega R \frac{R^2}{r^2} sin\theta \tag{S3}$$

where v_Ω is the angular velocity of the sphere and the relative velocity approaches bulk values as $1/r^2$. Because the solvent velocity field around a rotating sphere decays as $1/r^2$,

but decays as 1/*r* around a translating sphere, the viscous energy dissipation must occur in a thinner shell around a rotating sphere. This results in an apparent *increased* effect of the solvation water on rotational diffusion and must be compensated appropriately when calculating hydrated radii for rotational diffusion.

1.4 The effects of shape are different for translational and rotational diffusion

Most proteins are not perfectly spherical in shape and it is common to model this non-sphericity with ellipsoids, either ellipsoids of revolution where two axes are identical or general tri-axial ellipsoids where all three axes may be of different lengths. For identical volumes, an ellipsoid will have more surface area compared to a sphere and will have greater friction during diffusion. Analytical expressions for the dependence of the diffusional frictional coefficient on the axial ratio of ellipsoids of revolution have been worked out for both translational diffusion (14) and rotational diffusion (15, 16). For translational diffusion, the friction is averaged over random orientations of the ellipsoid and, for example, an axial ratio of 3 results in a ~10% increase in the frictional coefficient; similar effects are observed for both prolate and oblate ellipsoids with axial ratios <10 where the difference between prolate and oblate ellipsoids is 5.5%.

For rotational diffusion, the situation is more complex. There are two frictional coefficients, one for rotation about the major axis and one for rotation about the minor axis. The dependence of these coefficients on axial ratios is significantly different for prolate and oblate ellipsoids and the rotational frictional coefficients are generally greater than the translational coefficients. In the case of rotational diffusion, axial ratios of only 1.5 result in significant increases in friction (17). For elongated molecules, the rotational diffusion is better described by anisotropic tumbling rather than axially symmetric tumbling. Although it is not possible to analytically define a single rotational frictional coefficient, the practical outcome is that for NMR data analysis of small monomeric proteins an axially symmetric model is sufficient to describe the measured tumbling (6). Such a simplification may not be accurate for multi-domain proteins or very elongated structures. Therefore, as stated in the main text, the HullRad program prints a warning to the user concerning rotational properties if the axial ratio of a particular molecule is greater than that tested here by comparison to experimental data (a/b=2.62).

2 Supplemental Figures

2.1 Supplemental Figure 1

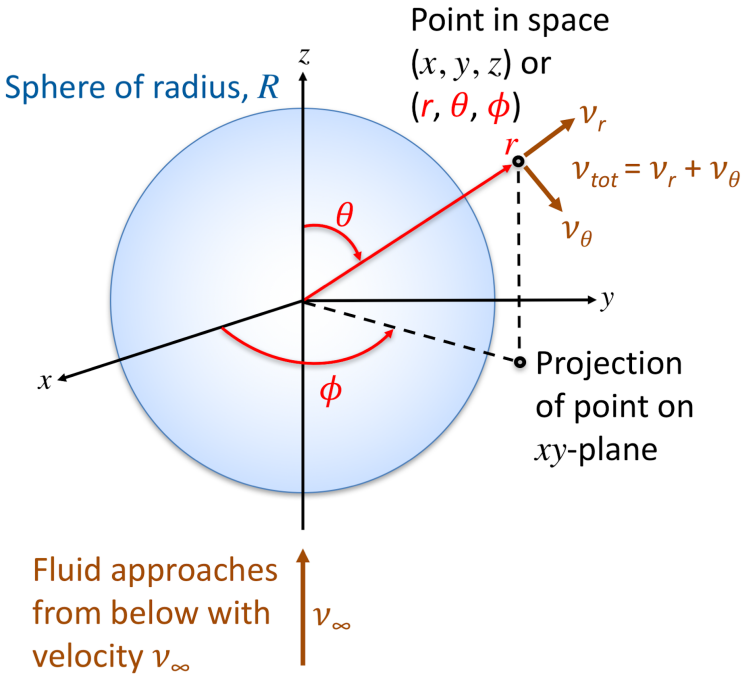

Supplemental Figure 1. Solvent velocity components around a sphere for flow at low Reynolds number. Here the fluid is flowing around a stationary sphere but the relative relationships are general and applicable to the case of a sphere diffusing in a stationary fluid. Adapted from (13). This figure was created in Microsoft PowerPoint.

2.2 Supplemental Figure 2

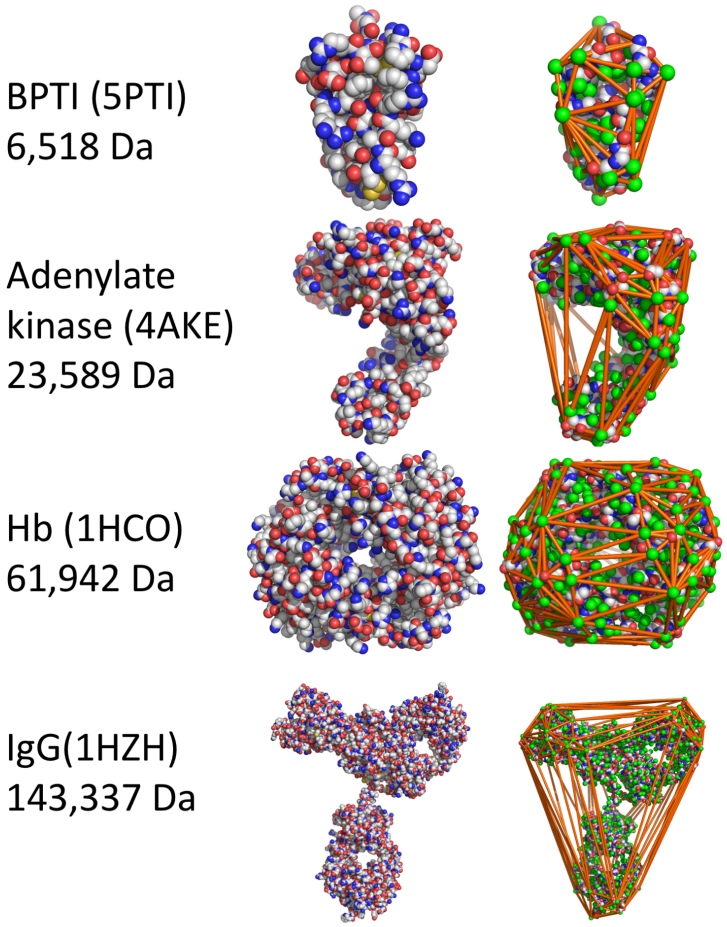

Supplemental Figure 2. Representation of the pseudo-atom side chain protein model. Left column: common name, PDB file and molecular mass; Middle column: atomic sphere representations; Right column: Unified atom side chain model (green side chain pseudo-atoms) with convex hull edges (orange sticks). Vertices of the convex hull are at the centers of the outer-most backbone atoms and side chain pseudo-atoms of the model.

2.3 Supplemental Figure 3

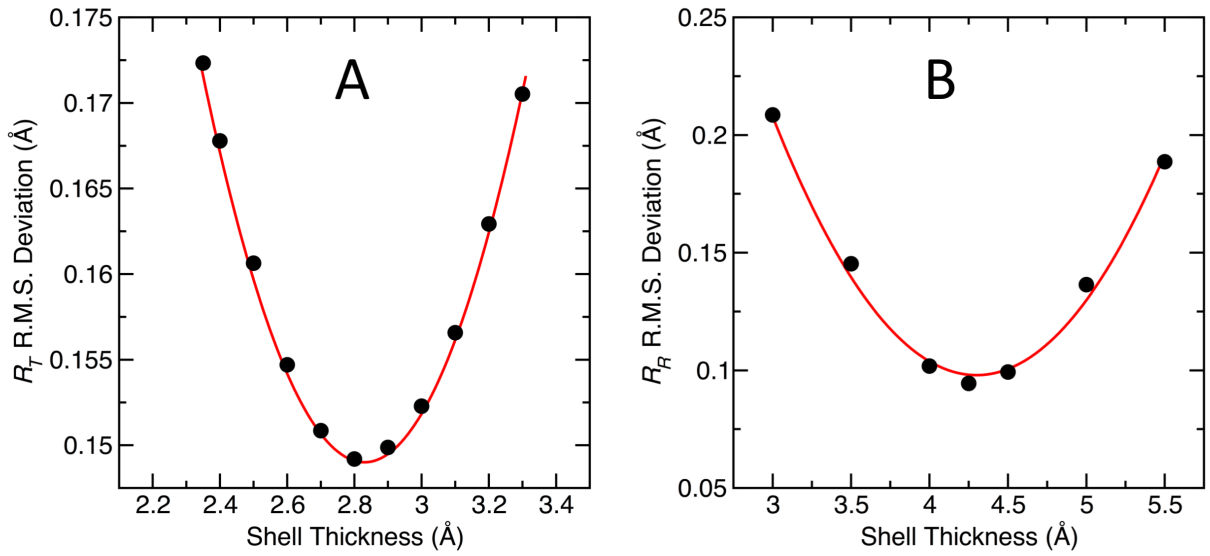

Supplemental Figure 3. Optimization of the hull expansion value to account for hydration. A. Translational hydrodynamic radii (R_T) corrected with a prolate ellipsoidal shape factor (F_T) were calculated for the proteins listed in Table 1 and the root mean squared deviations of convex hull to experimental values for different hydration shell thicknesses are shown as black circles. The data were fit to a quadratic expression (red line) and the minimum deviation is obtained at 2.83 Å shell thickness. B. Rotational hydrodynamic radii (R_R) corrected with a prolate ellipsoidal shape factor ($F_R = F_T^4$) were calculated for the proteins listed in Table 2 and the root mean squared deviations of convex hull to experimental values for different hydration shell thicknesses are shown as circles. The data were fit to a quadratic expression (red line) and the minimum deviation is obtained at 4.30 Å shell thickness.

2.4 Supplemental Figure 4

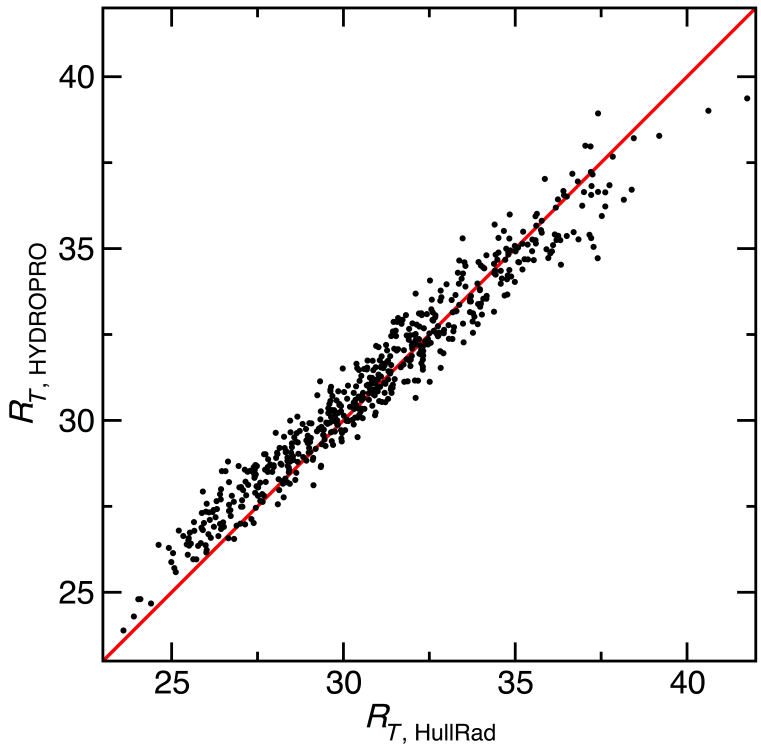

Supplemental Figure 4. Comparison of the effective translational hydrodynamic radii of disordered state ensemble protein structures calculated by HullRad and HYDROPRO. The red line represents a slope of one and intercept of zero; the correlation coefficient, *R*, for a linear regression of the data (not shown) is 0.95. The HYDROPRO hydrodynamic radii are, on average, ~0.7% larger than the HullRad hydrodynamic radii, but this is largely due to larger predicted values for compact structures. The ensemble contains 575 generated structures of α-synuclein from the Protein Ensemble Database (Accession number PED9AAC).

2.5 Supplemental Figure 5

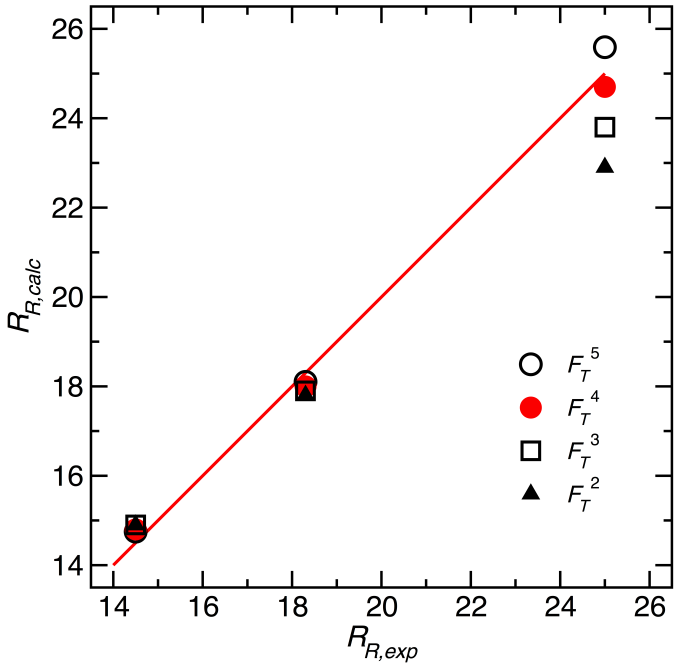

Supplemental Figure 5. Comparison of calculated to experimental R_R using different rotational shape factors. The rotational hydrodynamic radius (R_R) was calculated using HullRad with different rotational shape factors as follows: Open circles, $F_R = F_T^5$; red solid circles, $F_R = F_T^4$; open square, $F_R = F_T^3$; solid triangle, $F_R = F_T^2$. The red line represents a slope of one and intercept of zero. The plotted data are from Supplemental Table 1.

3 Supplemental Tables

3.1 Supplemental Table 1

Shape Factor Correction for Rotational Diffusion[a]

DNA Duplex	$R_{R,\text{exp}}$	$R_{R,\text{calc}}{}^{b}$ $F_T{}^{5}$	$R_{R,\text{calc}}{}^{c}$ $F_T{}^{4}$	$R_{R,\text{calc}}{}^{d}$ $F_T{}^{3}$	$R_{R,\text{calc}}{}^{e}$ $F_T{}^{2}$	Axial Ratio[f]
8mer	14.5	14.8	14.8	14.9	15.0	1.13
12mer	18.3	18.1	18.0	17.9	17.8	1.61
20mer	25.0	25.6	24.7	23.8	22.9	2.62

[a]The rotational hydrodynamic radii for three DNA duplexes were calculated with different rotational shape factors. In each case the optimal hydration shell expansion was determined for the specific shape factor using the protein data set listed in Table 2 in the main text in a manner similar to that shown in Supplemental Figure 3B.

[b]A shell expansion of 4.2 Å and shape factor equivalent to $F_T{}^{5}$ as the F_R was used.

[c]A shell expansion of 4.3 Å and shape factor equivalent to $F_T{}^{4}$ as the F_R was used.

[d]A shell expansion of 4.4 Å and shape factor equivalent to $F_T{}^{3}$ as the F_R was used.

[e]A shell expansion of 4.5 Å and shape factor equivalent to $F_T{}^{2}$ as the F_R was used.

[f]Axial ratio of a prolate ellipsoid of revolution with volume equal to convex hull volume of the molecule.

4 References

1. Kuntz, I. D., Jr., and W. Kauzmann. 1974. Hydration of proteins and polypeptides. Adv Protein Chem 28:239-345.
2. Aragon, S., and D. K. Hahn. 2006. Precise boundary element computation of protein transport properties: Diffusion tensors, specific volume, and hydration. Biophys J 91:1591-1603.
3. Garcia De La Torre, J., M. L. Huertas, and B. Carrasco. 2000. Calculation of hydrodynamic properties of globular proteins from their atomic-level structure. Biophys J 78:719-730.
4. Rocco, M., and O. Byron. 2015. Hydrodynamic Modeling and Its Application in AUC. Methods Enzymol 562:81-108.
5. Venable, R. M., E. Hatcher, O. Guvench, A. D. Mackerell, Jr., and R. W. Pastor. 2010. Comparing simulated and experimental translation and rotation constants: range of validity for viscosity scaling. J Phys Chem B 114:12501-12507.
6. Ryabov, Y. E., C. Geraghty, A. Varshney, and D. Fushman. 2006. An efficient computational method for predicting rotational diffusion tensors of globular proteins using an ellipsoid representation. J Am Chem Soc 128:15432-15444.
7. Kang, E. H., M. L. Mansfield, and J. F. Douglas. 2004. Numerical path integration technique for the calculation of transport properties of proteins. Phys Rev E Stat Nonlin Soft Matter Phys 69:031918.
8. Makarov, V. A., B. K. Andrews, P. E. Smith, and B. M. Pettitt. 2000. Residence times of water molecules in the hydration sites of myoglobin. Biophys J 79:2966-2974.
9. Denisov, V. P., and B. Halle. 1996. Protein hydration dynamics in aqueous solution. Faraday Discuss 103:227-244.
10. Halle, B., and M. Davidovic. 2003. Biomolecular hydration: from water dynamics to hydrodynamics. Proc Natl Acad Sci U S A 100:12135-12140.
11. Babick, F. 2016. Suspensions of Colloidal Particles and Aggregates. Springer International Publishing, Switzerland, 171.
12. Tanford, C. 1961. Physical Chemistry of Macromolecules. Wiley, New York, 337.
13. Bird, R. B., W. E. Stewart, and E. N. Lightfoot. 2002. Transport Phenomena. J. Wiley, New York,
14. Perrin, F. 1936. Mouvement Brownian d'un ellipsoide II. Rotation libre et dépolarisation des fluorescences. Translation et diffusion de molécules ellipsoïdales. Journal de Physique et Le Radium 7:1-11.
15. Edwardes, D. 1893. Steady motion of a viscous liquid in which an ellipsoid is constrained to rotate about a principal axis. The Quarerly Journal of Pure and Applied Mathematics 26:70-78.
16. Favro, L. D. 1960. Theory of the Rotational Brownian Motion of a Free Rigid Body. Phys Rev 119:53-62.
17. Cantor, C. R., and P. R. Schimmel. 1980. Biophysical Chemistry. Part II. Techniques for the study of biological structure and function. W. H. Freeman, New York, 561-565.